Nat. Hazards Earth Syst. Sci. Discuss., 3, 291–318, 2015
www.nat-hazards-earth-syst-sci-discuss.net/3/291/2015/
doi:10.5194/nhessd-3-291-2015

Natural Hazards and Earth System Sciences
Open Access
Discussions

PM_1 geochemical and mineralogical characterization using SEM-EDX to identify particle origin – Agri Valley pilot area (Basilicata, Southern Italy)

S. Margiotta[1,2], A. Lettino[1], A. Speranza[1], and V. Summa[1]

[1]Laboratory of Environmental and Medical Geology, CNR-IMAA, C. da S. Loja, Z.I., 85050 Tito Scalo (PZ), Italy
[2]Osservatorio Ambientale Val d'Agri, Via Vittorio Emanuele II, 3, 85052, Marsico Nuovo, Potenza, Italy

Received: 30 April 2014 – Accepted: 7 November 2014 – Published: 8 January 2015

Correspondence to: S. Margiotta (salvatore.margiotta@imaa.cnr.it)

Published by Copernicus Publications on behalf of the European Geosciences Union.

Abstract

A PM_1 geochemical and mineralogical study using Scanning Electron Microscopy (SEM) was performed on a pilot site in the Agri Valley which is close to the oil pre-treatment plant (C.O.V.A) of the Europe's largest on-shore hydrocarbon reservoir. The study identified PM_1 geochemical and mineralogical characters in a period before, during and immediately after a burning torch flare event. The finer fraction ($D_{Fe} < 0.7$ µm) consisted mainly of secondary particles and soot. In the coarser fraction ($D_{Fe} \geq 0.7$ µm), natural particles originating from crustal erosion and soot were abundant. Fine quartz particles and lower Al/Si ratios are markers for desert dust origin, proving that a Saharan dust episode which occurred during the observation period played a significant role in supplying geogenic aerosol components to the PM_1. Largest amounts of ≥ 0.7 µm fraction particles observed on the day of flare event may be due to a greater supply of Saharan geogenic particles. Soot had been significantly increasing long before the flare event, suggesting that this increase is also related to other causes, although we cannot exclude a contribution from flaring. S-rich aerosol consisted mainly of mixed particles originating from deposition and heterogeneous nucleation of secondary sulfates on mineral dust. Only-S particles were identified in the ≥ 0.7 µm fraction following the flare event. These particles may be indicators of larger amounts of sulphur in the atmosphere.

1 Introduction

In recent years, there has been an increasing scientific interest in atmospheric pollution and its affects on human health. Such interest has focused on atmospheric aerosols and their formation, transformation, transportation and deposition processes. Atmospheric aerosols are composed of solid and liquid particles, originating from anthropogenic sources (such as industrial activities, urban traffic and domestic heating) and natural sources (such as wind erosion of soils, pollen, volcanic eruption and desert

NHESSD
3, 291–318, 2015

dust), which can impact negatively on the environment, air quality and human health (e.g. Migon et al., 1997; Sokolik and Toon, 1999; Nickovic, 2002; Pope et al., 2002, 2009; Moshammer and Neuberger, 2003; Jawad Al Obaidy and Joshi, 2006; Pope and Dockery, 2006; Middleton et al., 2008; Kleanthous et al., 2009; Klein et al., 2010; Nickovic et al., 2012; Paternoster et al., 2014).

In order to obtain a complete typological characterization of atmospheric aerosols and to assess their role in the environment, it is important to apply measurement and characterization methods integrating conventional techniques. Scanning Electron Microscopy with Energy-Dispersed Analysis (SEM-EDX) play a very important role, providing morphological, chemical and mineralogical data fundamental in understanding the formation mechanisms of aerosols and distinguishing between natural and anthropogenic origin.

A PM_1 geochemical and mineralogical characterization was carried out using SEM, in a pilot site in the Agri Valley, to distinguish between the natural and anthropogenic origin of the finer atmospheric aerosols in an area of great environmental concern due to the presence of the largest European on-shore reservoir and an oil pre-treatment plant. In order to identify anomalies in the geochemical and mineralogical characters of the particles, observations were carried out from 22 September to 1 October 2012, before, during and immediately after a burning torch flare event on 28 September 2012.

The study focused on PM_1 as it is widely studied and recognized as a primarily anthropogenic aerosol, and its composition can be considered a good indicator of atmospheric pollution derived from SO_2 emissions (e.g. Nazaroff et al., 1990; Morawska et al., 1998; Wehner et al., 2002; Wiedensdohler et al., 2002; Alastuey et al., 2004; Monkonnen et al., 2005; Morawska et al., 2008; Weinzierl et al., 2009). Moreover, it is thought to be less affected by natural windblown dust than PM_{10} and $PM_{2.5}$ (e.g. Haller et al., 1991; Claiborn et al., 2000; Kegler et al., 2001).

NHESSD
3, 291–318, 2015

2 Pilot site

The pilot site (40°20′8″ N, 15°54′7″ E, 844 m a.s.l.) is located in the village of Viggiano (Potenza, Southern Italy), in the vicinity of C.O.V.A., a source of anthropogenic emissions located in the bottom of the valley, more than 200 m downstream (Fig. 1). There are also some industrial settlements nearby, the surrounding zones are mainly rural, agricultural activities are prevalent and there are extended woodlands and pastures in middle-mountains, partially protected by the Appennino Lucano – Val d'Agri – Lagonegrese National Park. The area has local road networks, modest traffic volumes, and a busier motorway (S.S. 598) linking the Agri Valley with the cities of Potenza and Taranto. This sampling site was chosen as Viggiano is the most populated town in the area, making it a more representative site with respect to potential risk for human health. Some key meteorological parameters were also available, such as atmospheric pressure, temperature, relative humidity and precipitations, which were provided by the Viggiano Civil Protection weather station.

The site has a mountain climate influenced by Mediterranean atmospheric circulation, resulting in dry summers and cold winters with precipitation concentrated in autumn and winter. This high rainfall is due to a proximity to the southwest Lucanian Apennine mountains, one of the wettest zones in Basilicata due to its exposure to Atlantic humid currents (Basilicata Region, 2006).

From 22 September to 1 October 2012, the weather station recorded average temperatures between 18.6 and 25.6 °C, with a peak of 30.9 °C on 29 September. There was no rainfall and average relative humidity ranged between 26 and 62 % (Fig. 2). During this period the Mediterranean Basin also experienced a dust episode, affecting the studied area (Fig. 3).

NHESSD
3, 291–318, 2015

3 Sampling, SEM-EDX analysis procedures and settings

As reported in Caggiano et al. (2010), PM_1 samples were collected using a low-volume gravimetric sampler equipped with a PM_1 cut-off inlet and polycarbonate filters. Sampling time was 24 h (starting from 12 p.m.). Each filter was humidity-conditioned in a filter-conditioning cabinet ($T = 20 \pm 2\,^{\circ}C$ and $RH = 50 \pm 5\,\%$) for 48 h, before and after sampling.

Microscopic analyses were carried out using a Field Emission Scanning Electron Microscope (FESEM, Zeiss Supra 40) equipped with an Energy Dispersive X-ray Spectrometer (EDX, Oxford Instruments). Portions of filter (about 0.5 cm^2) were attached to aluminum stubs (diameter 12 mm) using carbon sticky tabs and subsequently carbon coated. SEM images were obtained using both secondary (SE) and back-scattered (BSE) electrons. X-ray analyses were carried out using an energy-dispersive Si(Li) detector able to detect elements with $Z \geq 5$, nevertheless carbon and oxygen were not taken into account because they are components of polycarbonate substrate and carbon is used for coating the samples. Elemental composition characterization of particles was performed using the Inca Energy 350 Suite software.

Morphological and chemical analyses of particles were performed both manually and automatically. Automatic analyses were possible when an intense and clear signal was collected by BSE. By considering the Feret diameter (D_{Fe}), used for determining particle sizes (Merkus, 2009), finer particles ($D_{Fe} < 0.7\,\mu m$) were excluded due to the very weak image provided by the detector, and were only manually analyzed. On coarser particles ($D_{Fe} \geq 0.7\,\mu m$) automatic analyses were carried out by using Inca Feature software, presetting a BSE intensity threshold and using the following instrument parameters: working distance of 8.5 mm, acceleration voltage of 20 kV, aperture size of 60 µm and magnification of 15 000 ×. X-ray acquisition time was fixed at 20 s. The settings and area layout chosen allowed the detection and analysis, for each sample, of about 500 particles in random fields of view. Mamane et al. (2001) reported that physical and chemical properties of a sample can be well represented by analyzing several

NHESSD
3, 291–318, 2015

hundred particles. Accordingly, 500 particles detected were considered representative of the entire filters, showing a good homogeneous distribution of particulate. Elemental composition and morphological features of each particle were determined. The error associated with automated analysis, such as overlapping particles, contrast artifacts and sizing error, were corrected or eliminated by both manual off-line data review and manual data reacquisition from selected particles, in order to improve data quality.

Clustering of coarser particles ($D_{Fe} \geq 0.7$ µm) was carried out according to the rules indicated by Coz et al. (2009), with some modifications. In particular, we could distinguish between quartz (Si ≥ 90 %) and kaolinite (Si + Al ≥ 90 %), thanks to the use of polycarbonate filters instead of aluminium foils. The rules of Coz et al. (2009) were also considered in identifying sub-categories within the group of aluminosilicates (kaolinite, smectite and illite/mica). The average Al/Si ratio of the ≥ 0.7 µm fraction was calculated for each filter using the results of the particle elemental characterization. Particles without peaks in their X-ray spectra were reallocated and manually characterized in order to classify them from their morphological features.

Particle concentration on filter was also calculated as a ratio between the number of particles counted and the whole scanned surface.

Manual characterization of finer particles ($D_{Fe} < 0.7$ µm) was performed using SE images, reducing acceleration voltage to 15 kV and aperture size to 30 µm, and increasing magnification to 25 000 ×. About 300 particles were analyzed in each sample. This number is comparable to other studies carried out using the manual procedure (e.g. Paoletti et al., 1999; Ebert and Weinbruch, 2001; Lettino et al., 2012).

4 Results

The analyses performed allowed us to identify eight main types of particulate: silica particles, aluminosilicates, carbonates, biogenic particles, non biogenic C-rich particles, metal particles, S-rich particles and secondary particles with low-Z elements (Fig. 4). These particles were distributed differently in the ≥ 0.7 µm and < 0.7 µm fractions.

NHESSD
3, 291–318, 2015

Relative amounts of several particle typologies detected in the coarser fraction ($D_{Fe} \geq 0.7\,\mu m$) are shown in Fig. 5. Mineral component consisted of aluminosilicates, silica and carbonates, in this decreasing order.

Silica particles, composed of silica and oxygen alone, were represented by residual quartz (Fig. 4a). Silicates and aluminosilicates (Fig. 4b), the most abundant particles, were mainly composed of silica and aluminum, with variable amounts of calcium, magnesium, sodium, potassium, iron and titanium. For the most part, aluminosilicates consisted of clay minerals, with smectite $\gg$ kaolinite $>$ illite/mica (Fig. 6).

Carbonates included both calcite and dolomite. Calcite (Fig. 4c) was the more abundant phase, however dolomite was also well represented.

Mineral particles were often rounded because of wind erosion and long transport processes; clay particles preserved a plate morphology, but also showed crushed or chamfered edges linked to mechanical impacts due to mobilization and transport by wind.

Biogenic particles were mainly represented by pollens, brocosomes (Fig. 4d) and various types of organic fragments, with highly variable morphologies (e.g. plates, spores, column, etc.).

Non biogenic C-rich particles consisted of soot, cluster-like structures made up of a number of individual spheroids, with a diameter of a few tenths of a nanometre (30–50 nm), combined to form linear or branched-chain amorphous structures (Fig. 4e). Soot results from incomplete hydrocarbons combustion processes and forms at high temperatures by gas-to-particle conversion (e.g. Wolff, 1981; Han et al., 2010).

Metal particles were not frequent and were mainly composed of Fe and Ti. A smaller amount of Cr- and Pb-rich particles were also identified. A few metal particles detected (about 14 %) showed a spherical shape and were almost all composed of Fe or Pb (Fig. 4f).

The S-rich aerosol consisted mainly of polimineralic aggregates and mixed particles composed of secondary regular crystals of calcium sulfates grown directly onto Ca-rich particles (mainly carbonates) and sulfur compounds coating preexisting particles.

NHESSD
3, 291–318, 2015

Calcium sulfates were also present as residual gypsum (Fig. 4g). Smaller amounts of sodium sulfates, potassium sulfates and barium sulfates were recognized. A few droplet shaped particles counting only S (following OSP) were also identified.

In the finer fraction (DFe < 0.7 µm), particles with low-Z elements (i.e. C, N, O) were prevalent, such as soot and droplet shaped ammonium nitrates (Fig. 4h). Secondary phases represented by amorphous or droplet shaped particles, in which the EDX microanalysis detected only sulfur and/or sodium (ammonium sulfates, sodium nitrates, sodium sulfates or their mixtures) were also observed.

Mineral component of the aerosol is less abundant than that observed in the ≥ 0.7 µm fraction, with no change in composition: aluminosilicates, silica particles and carbonates were present in decreasing order. EDX spectra of these particles sometimes show a small peak in sulfur. Calcium sulfates were also present as residual gypsum.

5 Discussion

The ≥ 0.7 µm and < 0.7 µm particle size fractions show very different compositional characters with respect to the distribution of natural and anthropogenic components.

In the coarser fraction (D_{Fe} ≥ 0.7 µm) anthropogenic component consists mainly of soot. A few metal particles detected show a spherical morphology unequivocally indicative of an anthropogenic origin associated with combustion processes. The remaining metal particles (mainly iron or titanium oxides), show an irregular shape which did not allow the identification of origin.

Natural component is dominated by geogenic particles, originating from crustal erosion. They are composed of aluminosilicates (mainly clay minerals), quartz and carbonates (calcite and dolomite), in decreasing amount order. These mineral phases are consistent with lithological and pedological characters in the pilot area, characterized by soils on calcareous, marly or arenaceous substrates, moderately evolved by brunification and removal of carbonates (Basilicata Region, 2006). Biogenic particles (e.g. pollens, vegetable fragments, brocosomes) also contribute to the natural component.

NHESSD
3, 291–318, 2015

As shown in Fig. 7, S-rich aerosols consist mainly of mixed particles with a composed origin, as it can originate from deposition and heterogeneous nucleation (Kandler et al., 2007) of secondary sulfates (anthropogenic component) on mineral dust (natural component). Formation of $CaSO_4$ regular crystals accreted upon the surface of the pre-existing carbonate phases can result from interaction between H_2SO_4 and rich-Ca mineral particles (mainly carbonates), according to the following reaction (Harrison and Kitto, 1990; Clarke and Karani, 1992; Zhuang et al., 1999; Alastuey et al., 2004):

$$H_2SO_{4(aq,g)} + CaCO_{3(s)} \rightarrow CaSO_{4(s)} + H_2O + CO_{2(g)}. \quad \text{(R1)}$$

A geogenic S-rich component, represented by residual gypsum, is also present in minor amounts. This phase is a constituent of desert soil (Schwikowski et al., 1995; Claquin et al., 1999) and it is supposedly linked to a Saharan dust episode rather than an autochthonous contribution, hardly justifiable in the light of the lithologies outcropping in the area. Conversely, the OSP consist of secondary sulfur compounds of anthropogenic origin.

Total particle surface concentrations are reported in Fig. 8a. The largest amounts of particles in the coarser fraction were observed on 28 September 2012, due to increased geogenic particle quantities (Fig. 8b). Indeed, the dry deposition of crustal particles seems to make a significant contribution to the PM_1 accumulation on the filters, limited to the $\geq 0.7\,\mu m$ fraction.

As shown in Fig. 7, highest values of S-rich particle surface concentration were detected on the day of the flare, due to a significant increase in mixed particles. This increase is probably favoured by larger amounts of crustal particles that serve as substrate to nucleation or deposition of secondary sulphates.

Highest values of gypsum particles were detected on 24 September and 28 September, allowing the hypothesis that the Saharan dust episode influenced the PM_1 sampled on these dates, which also show a relative and absolute peak of geogenic particles respectively (Fig. 8b). Furthermore, these particles often have rounded morphologies or chamfered edges, and consist mainly of clay minerals (smectite, kaolinite and illite/mica

NHESSD
3, 291–318, 2015

in variable proportions) and quartz, which are the main components of atmospheric Saharan dust (e.g. Krueger et al., 2004; Brooks et al., 2005; Coz et al., 2009; Kandler et al., 2009). Particularly, on these dates the highest amounts of quartz were detected (Figs. 5 and 6), in accordance with the high mechanical stability of this mineral phase.

Average Al/Si ratios for each sample are consistently close to the value of 0.3, with lowest values on 24 September and 28 September (respectively 0.23 and 0.24, Fig. 9).

Al/Si ratios > 0.3 are generally considered indicators of desert dust (Molinaroli et al., 1996; Guerzoni et al., 1997; Blanco et al., 2003; Kandler et al., 2007; Matassoni et al., 2011), however Coude-Gaussen et al. (1987) have already found that the Al/Si ratio can vary with particle size. They noted that finest fractions have an Al/Si ratio significantly lower than that of mean aerosols, with values below 0.3, due to larger amounts of quartz. These fine quartz particles seem to be good indicators of aeolian and desert dust, because their formation can be attributed to impacts between sand grains (Krinsley and MacCoy, 1978), crystalline rock wind corrosion (Wilding et al., 1977) and amorphization of grains (Le Ribault, 1971, 1977), related to saltation and rolling aeolian mobilization. These processes are very efficient in desert areas, due to the absence of vegetation.

In the light of these considerations, the Al/Si ratios detected are in accordance with the assumption that the Saharan episode, particularly on 24 and 28 September, had a significant influence on the PM_1. A wind mark on the quartz particles was made on their morphological characters: they are often very "worked", with rounded corners and microfeatures probably originating from impacts during long periods of transport.

As shown in Fig. 8c, the highest soot surface densities on the filters was identified on the day after the flare at C.O.V.A. However, soot amounts had been significantly increasing since 25 September, long before the event, suggesting that this increase is related to different causes, such as long range transport, although we cannot exclude a soot contribution from flaring.

NHESSD
3, 291–318, 2015

Greatest amounts of OSP were detected on the filter of the day following the flare event. These particles may be indicators of larger amounts of sulphur in the atmosphere.

The finer particles ($D_{Fe} < 0.7\,\mu m$) consist mainly of anthropogenic or composite origin aerosols (soot and secondary particles such as ammonium sulfates, sodium nitrates, sodium sulfates or their mixtures), whereas natural component is much less significant than that in the coarser fraction.

Origin of secondary compounds can be attributed to different formation mechanisms.

Ammonium sulfates are the product of reaction between sulfuric acid and ammonia, which is the preferential reaction in the atmosphere (Korhonen et al., 1999; Kuhns et al., 2003; Baek et al., 2004; Almeida et al., 2005; Alastuey et al., 2004; Kandler et al., 2007; Vester et al., 2007).

Sodium nitrates could originate from the Reaction (R2) between sea salt and gaseous nitric acid (Savoie and Prospero, 1982; Harrison and Pio, 1983; Harrison et al., 1994; Finlayson-Pitts and Hemminger, 2000; Laskin et al., 2002).

$$HNO_{3(g)} + NaCl_{(s,aq)} \rightarrow NaNO_{3(s,aq)} + HCl_{(g)}. \quad \text{(R2)}$$

The supply of sea salt could be related to the pathways of air mass coming from North Africa across the Mediterranean Sea. Only a few unprocessed sea salt particles were detected, probably due to nitrates quickly replacing chloride (e.g. Laskin et al., 2002). Furthermore, the behavior of the hygroscopic NaCl particles can encourage aggregation with silicate particles, abundant in Saharan dust outbreaks (Levin et al., 2005; Matassoni et al., 2011).

The origin of sodium sulfates can be attributed to an analogous mechanism, ruled by the Reaction (R3) between H_2SO_4 and NaCl (Savoie and Prospero, 1982; Harrison and Pio, 1983; Querol et al., 1998; Meszaros, 1999; Zhuang et al., 1999; Alastuey et al., 2004)

$$H_2SO_{4(aq)} + 2NaCl_{(aq,s)} \rightarrow Na_2SO_{4(aq,s)} + 2HCl_{(g)}. \quad \text{(R3)}$$

NHESSD
3, 291–318, 2015

Wind erosion from saline dry lakes (Garrett, 2001) might contribute to a geogenic sodium sulfate component.

6 Conclusions

The pilot site's PM_1 contains a significant allochthonous component. Fine quartz particles and lower Al/Si ratios represent good markers for a desert dust origin, proving that Saharan dust episodes can play a significant role in supplying geogenic aerosol components to the PM_1. Therefore, studies of mineral dust and its influence on atmospheric processes, terrestrial environment and human health should not be neglected in this fraction.

Soot is the main anthropogenic component in the $\geq 0.7\,\mu m$ fraction. However, it's not possible to identify a certain cause–effect relationship between soot increment and flaring, because this increase started long before the event and could also be due to the Saharan dust episode which supplies allochthonous soot particles.

Deposition and heterogeneous nucleation of secondary sulfates on mineral dust and formation of composed origin (natural and anthropogenic) particles are very important mechanisms during the period studied, due to the presence in the atmosphere both of sulfur compounds and of geogenic substrates. Furthermore, the reactions of sulfur and nitrogen compounds with dust particles can be considered an important removal mechanism of SO_2 gaseous pollutants and their reaction products present in the atmosphere. This removal mechanism due to dust particles was already indicated for the supermicrometer fractions by Kerminen et al. (1997) and Zhuang et al. (1999).

In the light of these considerations, and in agreement with Alastuey et al. (2005), it can be concluded that Saharan episodes mark the PM_1 composition with regard both to geogenic component and to soot amounts and secondary aerosols, also supplying allochthonous pollutants as already indicated by Formenti et al. (2011) and Rodriguez et al. (2011).

NHESSD
3, 291–318, 2015

The Saharan episode hides the identification of soot contribution to a flaring event, suggesting that soot autochthonous contribution in the pilot site, and in a "flaring condition", can be easily superceded by allochthonous soot carried by a Saharan episode, which frequently occur in the Mediterranean Basin. Conversely, the presence of OSP in the ≥ 0.7 fraction on the day after the flaring suggest these particles are a possible indicator of increased sulfur in the atmosphere.

Acknowledgements. This work is part of the research activities carried out at the Osservatorio Ambientale Val d'Agri, Marsico Nuovo (Potenza), with the support of Basilicata Region (Dipartimento Ambiente, Territorio e Politiche della Sostenibilità). The authors would like to thank Rosa Caggiano (CNR-IMAA) for making the filters available. We express our gratitude to Viggiano Civil Protection who provide meteorological data. The authors acknowledge the US Naval Research Laboratory for the contribution given by the information reported in NAAPS archive and used in this work.

References

Alastuey, A., Querol, X., Rodriguez, S., Plana, F., Lopez-Soler, A., Ruiz, C., and Mantilla, E.: Monitoring of atmospheric particulate matter around sources of secondary inorganic aerosol, Atmos. Environ., 38, 4979–4992, 2004.

Alastuey, A., Querol, X., Castillo, S., Escudero, M., Avila, A., Cuevas, E., Torres, C., Romero, P., Exposito, F., Garcia, O., Diaz, J. P., Van Dingenen, R., and Putaud, J. P.: Characterization of TSP and $PM_{2.5}$ at Izana and Sta. Cruz de Tenerife (Canary Islands, Spain) during a Saharan Dust Episode (July 2002), Atmos. Environ., 39, 4715–4728, 2005.

Almeida, S. M., Pio, C. A., Freitas, M. C., Reis, M. A., and Trancoso, M. A.: Source apportionment of fine and coarse particulate matter in a sub-urban area at the Western European Coast, Atmos. Environ., 39, 3127–3138, 2005.

Baek, B. H., Aneja, V. P., and Tong, Q.: Chemical coupling between ammonia, acid gases, and fine particles, Environ. Pollut., 129, 89–98, 2004.

Basilicata Region: I suoli della Basilicata. Carta pedologica della Regione Basilicata in scala 1 : 250 000, Note Illustrative, Regione Basilicata, Dipartimento Agricultura, Sviluppo Rurale, Economia Montana, Potenza, 341 pp., 2006.

NHESSD

3, 291–318, 2015

Blanco, A., Dee Tomasi, F., Filippo, E., Manno, D., Perrone, M. R., Serra, A., Tafuro, A. M., and Tepore, A.: Characterization of African dust over southern Italy, Atmos. Chem. Phys., 3, 2147–2159, doi:10.5194/acp-3-2147-2003, 2003.

Brooks, N., Chiapello, I., Lernia, S. D., Drake, N., Legrand, M., Moulin, C., and Prospero, J.: The climate-environment-society nexus in the Sahara from prehistoric times to the present day, J. North Afr. Stud., 10, 253–292, 2005.

Caggiano, R., Macchiato, M., and Trippetta, S.: Levels, chemical composition and sources of fine aerosol particles (PM_1) in an area of the Mediterranean Basin, Sci. Total Environ., 408, 884–895, 2010.

Claiborn, C. S., Finn, D., Koenig, J. Q., and Larson, T. V.: Windblown dust contributes to high $PM_{2.5}$ concentrations, J. Air Waste Manage., 50, 1440–1445, 2000.

Claquin, T., Schulz, M., and Balkanski, Y. J.: Modeling the mineralogy of atmospheric dust sources, J. Geophys. Res., 104, 22243–22256, 1999.

Clarke, A. G. and Karani, G. B.: Characterization of the carbonate content of atmospheric aerosols, J. Atmos. Chem., 14, 119–128, 1992.

Coude-Gaussen, G., Rognon, P., Bergametti, G., Gomes, L., Strauss, B., Gros, J. M., and Le Costumer, M. N.: Saharan dust on Fuerteventura Island (Canaries): chemical and mineralogical characteristics, air mass trajectories and probable sources, J. Geophys. Res., 92, 9753–9771, 1987.

Coz, E., Gomez-Moreno, F. J., Pujadas, M., Casuccio, G. S., Lersch, T. L., and Artinano, B.: Individual particle characteristics of North African dust under different long-range transport scenarios, Atmos. Environ., 43, 1850–1863, 2009.

Ebert, M. and Weinbruch, S.: High-resolution scanning electron microscopy of atmospheric particles sampled at Junfraujoch during the CLACE Field Experiment, Activity Report 1999/2000, International Foundation High Altitude Research Stations JG, Bern, Switzerland, 57–62, 2001.

Finlayson-Pitts, B. J. and Hemminger, J. C.: Physical chemistry of airborne sea salt particles and their component, J. Phys. Chem. A, 104, 11463–11477, 2000.

Formenti, P., Schütz, L., Balkanski, Y., Desboeufs, K., Ebert, M., Kandler, K., Petzold, A., Scheuvens, D., Weinbruch, S., and Zhang, D.: Recent progress in understanding physical and chemical properties of African and Asian mineral dust, Atmos. Chem. Phys., 11, 8231–8256, doi:10.5194/acp-11-8231-2011, 2011.

NHESSD

3, 291–318, 2015

Garrett, D. E.: Sodium Sulfate: Handbook of Deposits, Processing, & Use, Academic Press, London, UK, 2001.
Guerzoni, S., Molinaroli, E., and Chester, R.: Saharan dust input to the western Mediterranean Sea: depositional patterns, geochemistry and sedimentologic implications, Deep-Sea Res. Pt. II, 43, 631–654, 1997.
Haller, L., Claiborn, C., Larson, T., Koenig, J., Norris, G., and Edgar, R.: Airborne particulate matter size distributions in an arid urban area, J. Air Waste Manage., 49, 161–168, 1991.
Han, Y. M., Cao, J.J., Lee, S. C., Ho, K. F., and An, Z. S.: Different characteristics of char and soot in the atmosphere and their ratio as an indicator for source identification in Xi'an, China, Atmos. Chem. Phys., 10, 595–607, doi:10.5194/acp-10-595-2010, 2010.
Harrison, R. M. and Kitto, A.-M. N.: Field intercomparison of filter pack and denuder sampling methods for reactive gaseous and particulate pollutants, Atmos. Environ. A-Gen., 24, 2633–2640, 1990.
Harrison, R. M. and Pio, C. A.: Size-differentiated composition of inorganic atmospheric aerosols of both marine and polluted continental origin, Atmos. Environ., 17, 1733–1783, 1983.
Harrison, R. M., Msibi, M. I., Kitto, A.-M. N., and Yamulki, S.: Atmospheric chemical transformations of nitrogen compounds measured in the North Sea experiment, September 1991, Atmos. Environ., 28, 1593–1599, 1994.
Jawad Al Obaidy, A. H. M. and Joshi, H.: Chemical composition of rainwater in a tropical urban area of northern India, Atmos. Environ., 40, 6886–6891, 2006.
Kandler, K., Benker, N., Bundke, U., Cuevas, E., Ebert, M., Knippertz, P., Rodríguez, S., Schütz, L., and Weinbruch, S.: Chemical composition and complex refractive index of Saharan mineral dust at Izana, Tenerife (Spain) derived by electron microscopy, Atmos. Environ., 41, 8058–8074, 2007.
Kandler, K., Schutz, L., Deutscher, C., Ebert, M., Hofmann, H., Jackel, S., Jaenicke, R., Knippertz, P., Lieke, K., Massling, A., Petzold, A., Scladitz, A., Weinzierl, B., Wiedensohler, A., Zorn, S., and Weinbruch, S.: Size distribution, mass concentration, chemical and mineralogical composition and derived optical parameters of the boundary layer aerosol at Tinfou, Morocco, during SAMUM 2006, Tellus B, 61, 32–50, 2009.
Kegler, S. R., Wilson, W. E., and Marcus, A. H.: PM_1, intermodal ($PM_{2.5}$-1) mass, and the soil component of $PM_{2.5}$ in Phoenix, AZ, 1995–1996, Aerosol Sci. Tech., 35, 914–920, 2001.

NHESSD
3, 291–318, 2015

Kerminen, V. M., Pakkanen, T. A., and Hillamo, R. E.: Interactions between inorganic trace gases and supermicrometer particles at a coastal site, Atmos. Environ., 31, 2753–2765, 1997.
Kleanthous, S., Bari, M. A., Baumbach, G., and Sarachage-Ruiz, L.: Influence of particulate matter on the air quality situation in a Mediterranean island, Atmos. Environ., 43, 4745–4753, 2009.
Klein, H., Nickovic, S., Haunold, W., Bundke, U., Nillius, B., Ebert, M., Weinbruch, S., Schuetz, L., Levin, Z., Barrie, L. A., and Bingemer, H.: Saharan dust and ice nuclei over Central Europe, Atmos. Chem. Phys., 10, 10211–10221, doi:10.5194/acp-10-10211-2010, 2010.
Korhonen, P., Kulmala, M., Laaksonen, A., Viisanen, Y., McGraw, R., and Seinfeld, J. H.: Ternary nucleation of H_2SO_4, NH_3 and H_2O in the atmosphere, J. Geophys. Res., 104, 26349–26353, 1999.
Krinsley, D. H. and MacCoy, F.: Aeolian quartz sand and silt, in: Scanning Electron Microscopy in the Study of Sediments, Geoabstract, Norwich, England, 249–260, 1978.
Krueger, B. J., Grassian, V. H., Cowin, J. P., and Laskin, A.: Heterogeneous chemistry of individual mineral dust particles from different dust source regions: the importance of particle mineralogy, Atmos. Environ., 38, 6253–6261, 2004.
Kuhns, H., Bohdan, V., Chow, J. C., Etyemezian, V., Green, M. C., Herlocker, D., Kohl, S., Mc Gown, M., Ramsdell, J., Stockwell, W. R., Toole, M., and Watson, J.: The Treasure Valley secondary aerosol study I: measurements and equilibrium modeling of inorganic secondary aerosols and precursors for southwestern Idaho, Atmos. Environ., 37, 511–524, 2003.
Laskin, A., Iedema, M. J., and Cowin, J. P.: Quantitative time-resolved monitoring of nitrate formation in sea salt particles using a CCSEM/EDX single particle analysis, Environ. Sci. Technol., 36, 4948–4955, 2002.
Le Ribault, L.: Présence d'une pellicule de silice amorphe à la surface de cristaux de quartz des formations sableuses, Compterendus del l'Académie des Sciences, 272, 1933–1936, 1971.
Le Ribault, L.: L'exoscopie des quartz, Editions Masson, Epuisé, Paris, 200 pp., 1977.
Lettino, A., Caggiano, R., Fiore, S., Macchiato, M., Sabia, S., and Trippetta, S.: Eyjafjallajokull volcanic ash in southern Italy, Atmos. Environ., 48, 97–103, 2012.

NHESSD
3, 291–318, 2015

Levin, Z., Teller, A., Ganor, E., and Yin, Y.: On the interactions of mineral dust, sea salt particles and clouds – a measurement and modeling study from the MEIDEX campaign, J. Geophys. Res., 110, D20202, doi:10.1029/2005JD005810, 2005.

Mamane, Y., Willis, R., and Conner, T.: Evaluation of computer-controlled scanning electron microscopy applied to an ambient urban aerosol sample, Aerosol Sci. Tech., 34, 97–107, 2001.

Matassoni, L., Pratesi, G., Centioli, D., Cadoni, F., Lucarelli, F., Nava, S., and Malesani, P.: Saharan dust contribution to PM_{10}, $PM_{2.5}$ and PM_1 in urban and suburban areas of Rome: a comparison between single-particles SEM-EDX analysis and whole-sample PIXE analysis, J. Environ. Monitor., 13, 732–742, 2011.

Merkus, H. G.: Particle Size Measurements: Fundamentals, Practice, Quality, Particle Technology, Series 17, Springer, the Netherlands, 536 pp., 2009.

Meszaros, E.: Fundamentals of Atmospheric Aerosol Chemistry, Akademiai Kiado, Budapest, 308 pp., 1999.

Middleton, N., Yiallouros, P., Kleanthous, S., Kolokotroni, O., Schwartz, J., Dockery, D. W., Demokritou, P., and Koutrakis, P.: A 10 yr time-series analysis of respiratory and cardiovascular morbidity in Nicosia, Cyprus: the effect of short-term changes in air pollution and dust storms, Environ. Health, 7, 1–16, 2008.

Migon, C., Journel, B., and Nicolas, E.: Measurement of trace metal wet, dry and total atmospheric fluxes over the Ligurian Sea, Atmos. Environ., 16, 1701–1709, 1997.

Molinaroli, E.: Mineralogical characterization of Saharan dust with a view to its final destination in Mediterranean sediments, in: The Impact of Desert Dist across the Mediterranean, edited by: Guerzoni, S. and Chester, R., Kluwer Academic Publishers, Netherlands, 153–162, 1996.

Mönkkönen, P., Koponen, I. K., Lehtinen, K. E. J., Hämeri, K., Uma, R., and Kulmala, M.: Measurements in a highly polluted Asian mega city: observations of aerosol number size distribution, modal parameters and nucleation events, Atmos. Chem. Phys., 5, 57–66, doi:10.5194/acp-5-57-2005, 2005.

Morawska, L., Thomas, S., Bofinger, N., Wainwright, D., and Neale, D.: Comprehensive characterization of aerosols in a subtropical urban atmosphere: particle size distribution and correlation with gaseous pollutants, Atmos. Environ., 32, 2467–2478, 1998.

NHESSD

3, 291–318, 2015

Morawska, L., Keogh, D. U., Thomas, S. B., and Mengersen, K.: Modality in ambient particle size distributions and its potential as a basis for developing air quality regulation, Atmos. Environ., 42, 1617–1628, 2008.
Moshammer, H. and Neuberger, M.: The active surface of suspended particles as a predictor of lung function and pulmonary symptoms in Austrian school children, Atmos. Environ., 37, 1737–1744, 2003.
Nazaroff, W. W., Ligocki, M. P., Ma, T., and Cass, G. R.: Particle deposition in museums: comparison of modelling and measurement results, Aerosol Sci. Tech., 13, 332–348, 1990.
Nickovic, S.: Dust aerosol modelling: step toward integrated environmental forecasting, Eos. Trans. AGU, 83, Fall Meet., A71E-04, 2002.
Nickovic, S., Vukovic, A., Vujadinovic, M., Djurdjevic, V., and Pejanovic, G.: Technical Note: High-resolution mineralogical database of dust-productive soils for atmospheric dust modeling, Atmos. Chem. Phys., 12, 845–855, doi:10.5194/acp-12-845-2012, 2012.
Paoletti, L., Diociaiuti, M., De Berardis, B., Santucci, S., Lozzi, L., and Picozzi, P.: Characterisation of aerosol individual particles in a controlled underground area, Atmos. Environ., 33, 3603–3611, 1999.
Paternoster, M., Sinisi, R., Mancusi, C., Pilat, K., Sabia, A., and Mongelli, G.: Natural versus anthropogenic influences on the chemical composition of bulk precipitation in the southern Apennines, Italy: a case study of the town of Potenza, J. Geochem. Explor., 145, 242–249, 2014.
Pope, C. A. and Dockery, D. W.: Health effects of fine particulate air pollution: lines that connect, J. Air Waste Manage., 56, 709–742, 2006.
Pope, C. A., Burnett, R. T., Thun, M. J., Calle, E. E., Krewsky, D., Ito, K., and Thurston, G. D.: Lung cancer, cardiopulmonary mortality, and long-term exposure to fine particulate air pollution, J. Amer. Med. Assoc., 287, 1132–1141, 2002.
Pope, C. A., Ezzati, M., and Dockery, D. W.: Fine-particulate air pollution and life expectancy in the Unites States, New Engl. J. Med., 360, 376–386, 2009.
Querol, X., Alastuey, A., Lopez-Soler, A., Plana, F., Puicercus, J. A., Ruiz, C. R., Mantilla, E., and Juan, R.: Seasonal evolution of the atmospheric suspended particles around a coalfired power station: chemical characterization, Atmos. Environ., 32, 719–731, 1998.
Rodríguez, S., Alastuey, A., Alonso-Pérez, S., Querol, X., Cuevas, E., Abreu-Afonso, J., Viana, M., Pérez, N., Pandolfi, M., and de la Rosa, J.: Transport of desert dust mixed with

NHESSD
3, 291–318, 2015

North African industrial pollutants in the subtropical Saharan Air Layer, Atmos. Chem. Phys., 11, 6663–6685, doi:10.5194/acp-11-6663-2011, 2011.
Savoie, D. L. and Prospero, J. M.: Particle size distribution of nitrate and sulfate in the marine atmosphere, Geophys. Res. Lett., 9, 1207–1210, 1982.
Schwikowski, M., Seibert, P., Baltensperger, U., and Gaggeler, H. W.: A study of an outstanding Saharan dust event at the high-alpine site Jungfraujoch, Switzerland, Atmos. Environ., 29, 1829–1842, 1995.
Sokolik, I. and Toon, O.: Incorporation of mineralogical composition into models of the radiative properties of mineral aerosol from UV to IR wavelengths, J. Geophys. Res., 104, 9423–9444, 1999.
Vester, B. P., Ebert, M., Barnert, E., Schneider, J., Kandler, K., Schutz, L., and Weinbruch, S.: Composition and mixing state of the urban background aerosol in the Rhein main area (Germany), Atmos. Environ., 41, 6102–6115, 2007.
Wehner, B., Birmili, W., Gnauk, T., and Wiedensohler, A.: Particle number size distributions in a street canyon and their transformation into the urban-air background: measurements and a simple model study, Atmos. Environ., 36, 2215–2223, 2002.
Weinzierl, B., Petzold, A., Esselborn, M., Wirth, M., Rasp, K., Kandler, K., Schutz, L., Koepke, P., and Fiebig, M.: Airborne measurements of dust layer properties, particle size distribution and mixing state of Saharan dust during SAMUM 2006, Tellus B, 61, 96–117, 2009.
Wiedensohler, A., Wehner, B., and Birmili, W.: Aerosol Number Concentrations and Size Distributions at Mountain-Rural, Urban-Influenced Rural, and Urban-Background Sites in Germany, J. Aerosol Med., 15, 237–243, doi:10.1089/089426802320282365, 2002.
Wilding, L. P., Smeck, N. E., and Drees, L. R.: Silica in soils: quartz, cristobalite, tridymite and opal, in: Minerals in Soil Environments, edited by: Dixon, J. B., Weed, S. B., Kittrick, J. A., Milford, M. H., and White, J. L., Soil Science Society of America Inc. (SSSA), Madison, Wisconsin, 471–552, 1977.
Wolff, G. T.: Particulate elemental carbon in the atmosphere, JAPCA J. Air Waste Ma., 31, 935–938, 1981.
Zhuang, H., Chan, C. K., Fang, M., and Wexler, A. S.: Formation of nitrate and non sea-salt sulfate on coarse particles, Atmos. Environ., 33, 4223–4233, 1999.

NHESSD
3, 291–318, 2015

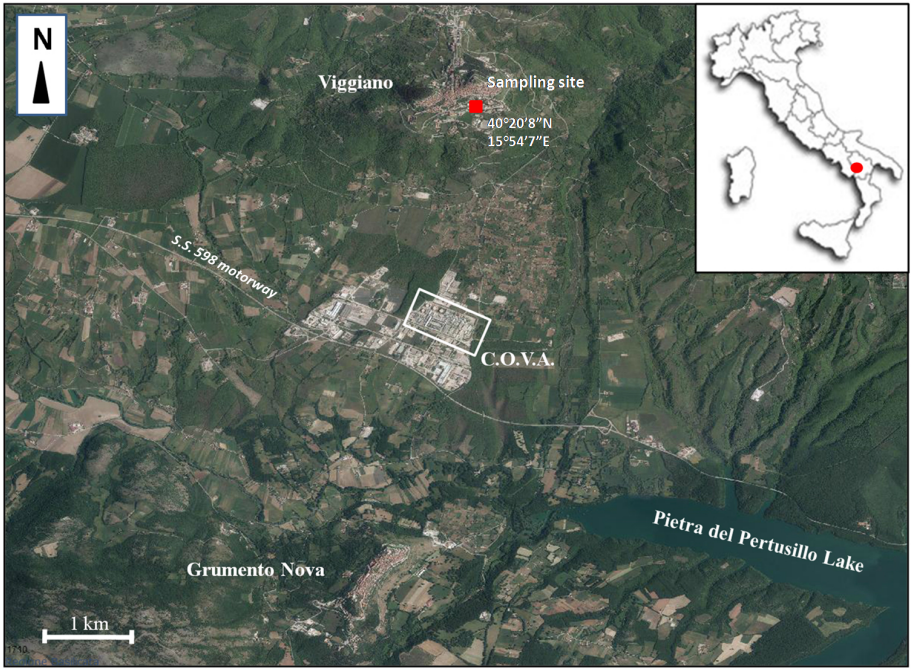

Figure 1. Location of the sampling site and Agri Valley pre-treatment plant (C.O.V.A). Copyright AGEA – Orthophoto 2011.

NHESSD
3, 291–318, 2015

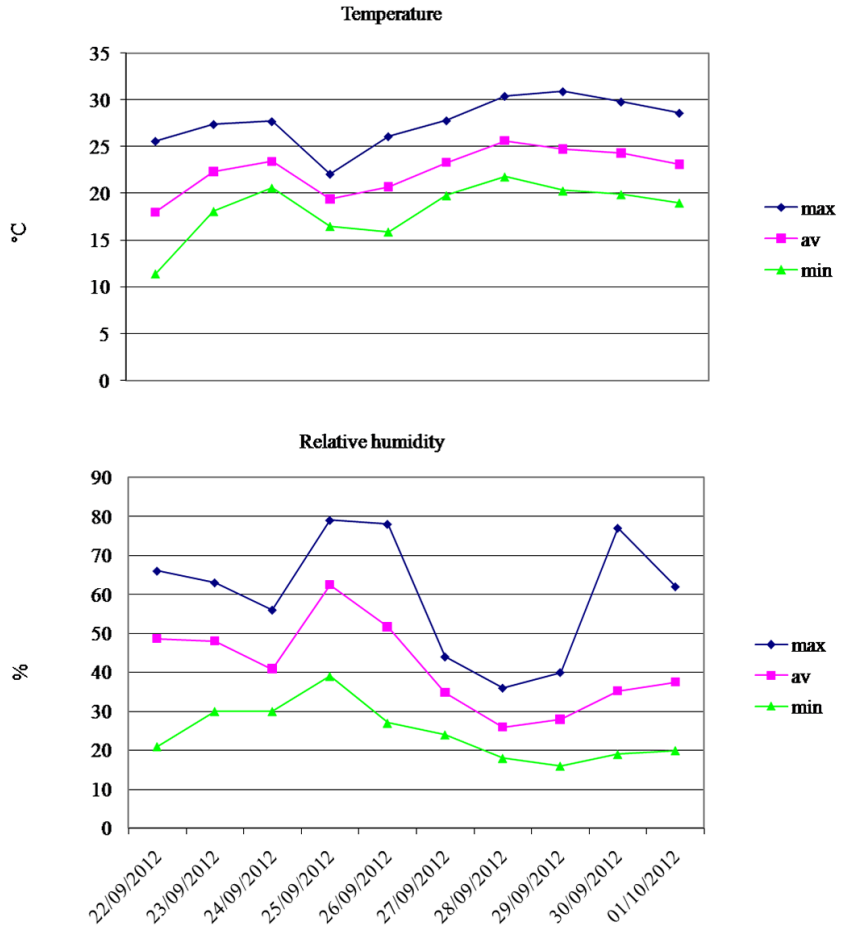

Figure 2. Temperature and relative humidity trends during the observation period at Viggiano Civil Protection weather station.

NHESSD
3, 291–318, 2015

PM$_1$ geochemical and mineralogical characterization using SEM-EDX

S. Margiotta et al.

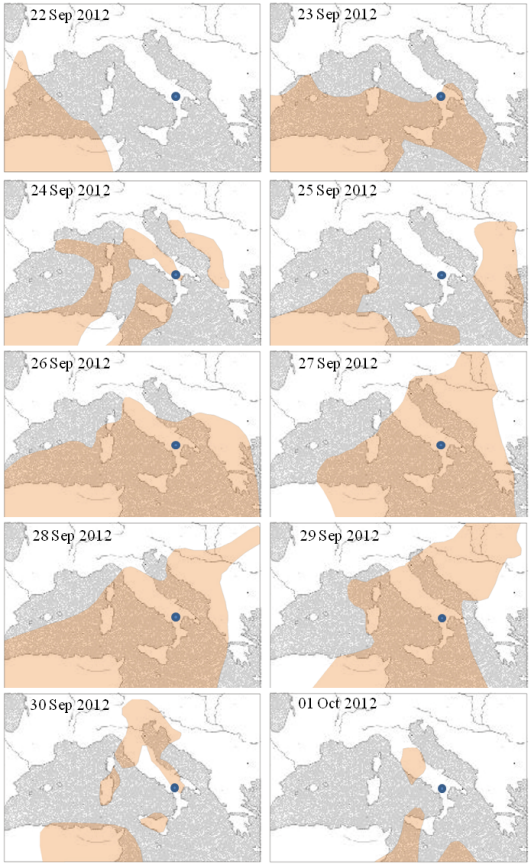

Figure 3. Sketch maps of the Mediterranean Basin highlighting areas with Dust Surface Concentrations $\geq 20\,\mu g\,m^{-3}$ at 12:00 UTC, from NAAPS (Navy Aerosol Analysis and Prediction System) Archive of US Naval Research Laboratory (http://www.nrlmry.navy.mil/aerosol/), modified.

NHESSD
3, 291–318, 2015

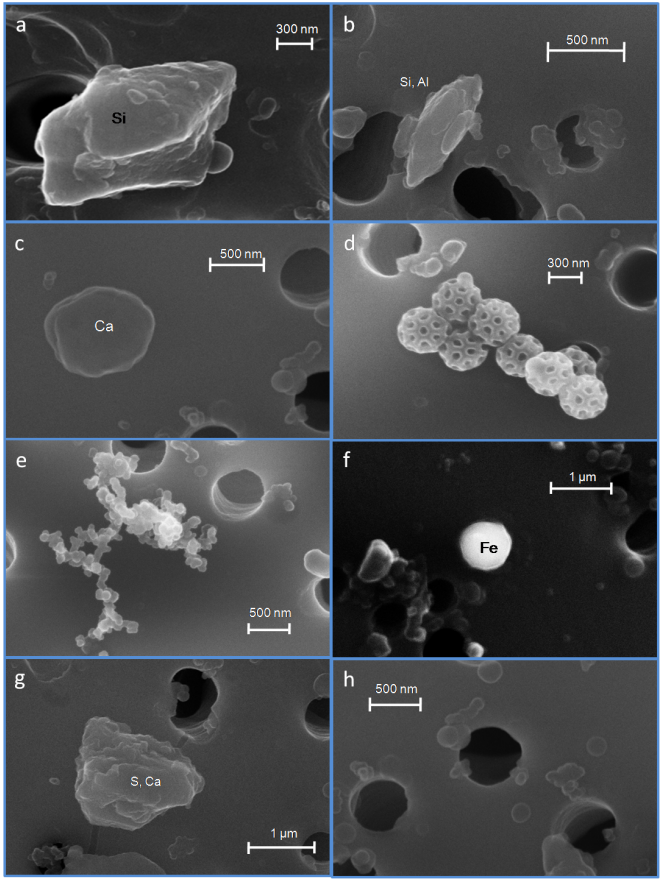

Figure 4. SEM images of each main typology of particles identified: **(a)** silica particle (quartz); **(b)** aluminosilicate (kaolinite); **(c)** carbonate particle (calcite); **(d)** biogenic particle (brocosomes); **(e)** non biogenic C-rich particle (soot); **(f)** metal particle (iron oxide); **(g)** S-rich particle (gypsum); **(h)** secondary low-Z element particles.

NHESSD
3, 291–318, 2015

PM$_1$ geochemical and mineralogical characterization using SEM-EDX

S. Margiotta et al.

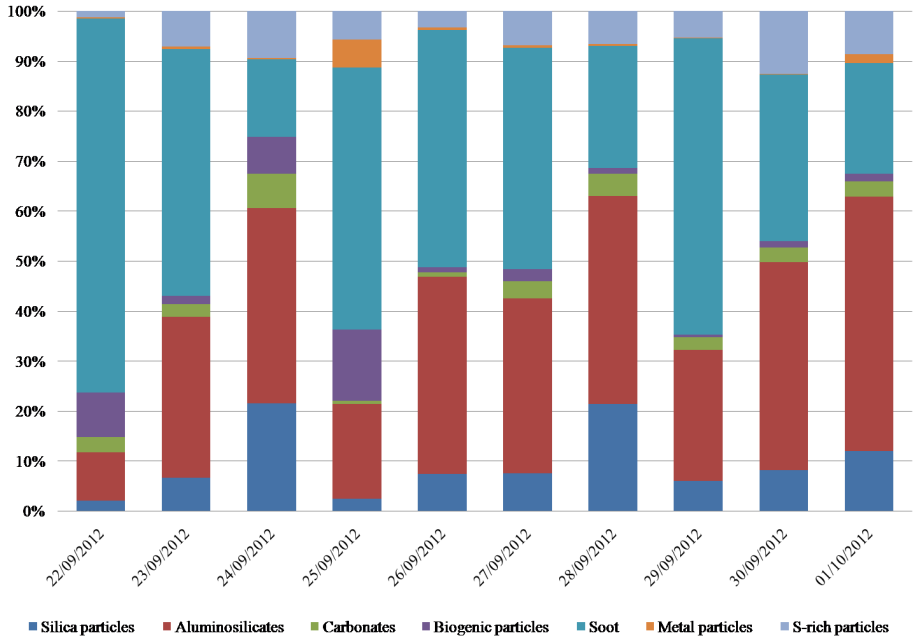

Figure 5. Numerical relative amounts (%) of several particle typologies identified in the ≥ 0.7 µm fraction.

NHESSD
3, 291–318, 2015

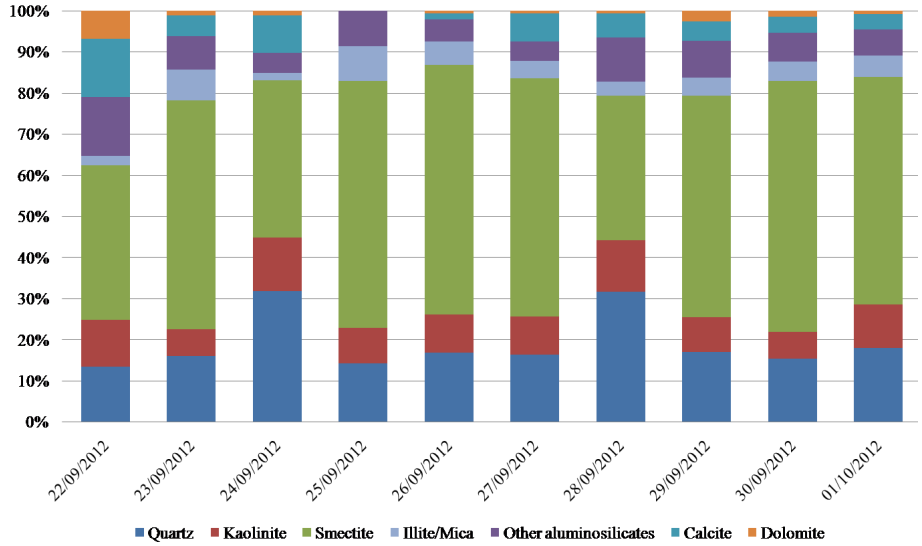

Figure 6. Numerical relative amounts (%) of the phases composing the mineral component in the ≥ 0.7 µm fraction.

NHESSD
3, 291–318, 2015

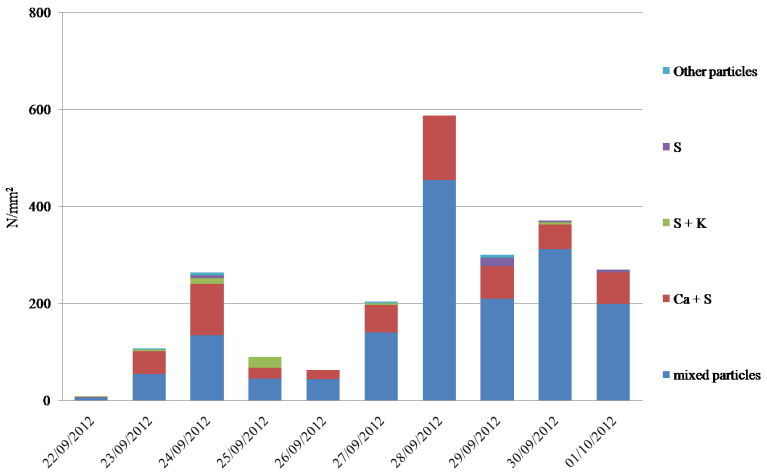

Figure 7. Surface concentration of several S-rich particulate components in the ≥ 0.7 µm fraction.

NHESSD
3, 291–318, 2015

PM$_1$ geochemical and mineralogical characterization using SEM-EDX

S. Margiotta et al.

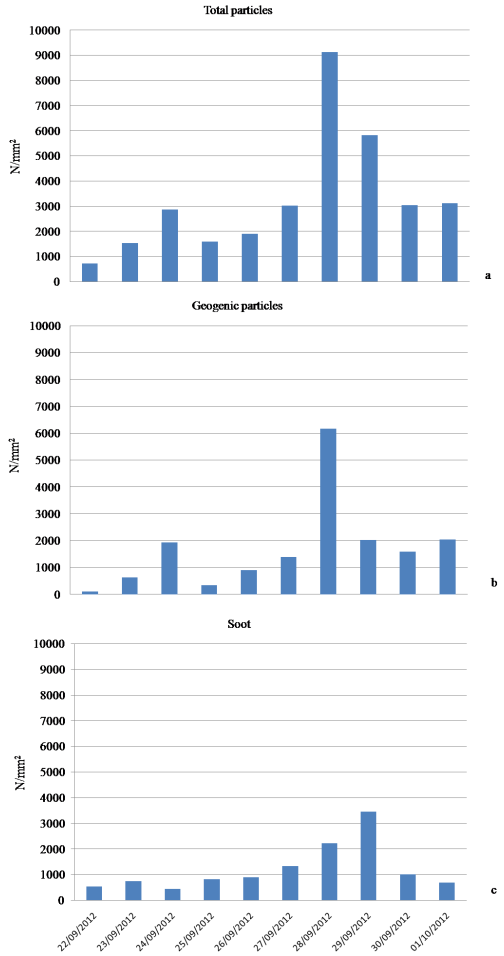

Figure 8. Surface concentration trends of total particles **(a)**, geogenic particles **(b)** and soot **(c)** in the ≥ 0.7 µm fraction.

NHESSD
3, 291–318, 2015

PM$_1$ geochemical and mineralogical characterization using SEM-EDX

S. Margiotta et al.

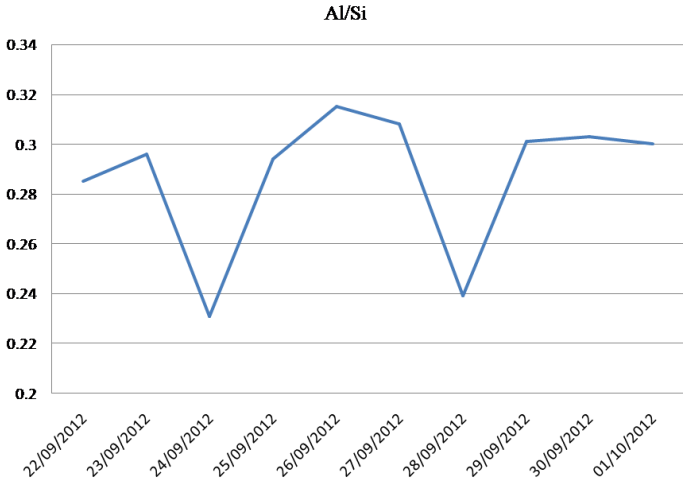

Figure 9. Al/Si ratio trend.

NHESSD
3, 291–318, 2015

PM$_1$ geochemical and mineralogical characterization using SEM-EDX

S. Margiotta et al.